The Cytoplasmic Tail of Rhodopsin Acts as a Novel Apical Sorting Signal in Polarized MDCK Cells

Jen-Zen Chuang* and Ching-Hwa Sung*‡

*Department of Ophthalmology, ‡Department of Cell Biology and Anatomy, The Margaret M. Dyson Vision Research Institute, Cornell University Medical College, New York 10021

Abstract. All basolateral sorting signals described to date reside in the cytoplasmic domain of proteins, whereas apical targeting motifs have been found to be lumenal. In this report, we demonstrate that wild-type rhodopsin is targeted to the apical plasma membrane via the TGN upon expression in polarized epithelial MDCK cells. Truncated rhodopsin with a deletion of 32 COOH-terminal residues shows a nonpolar steady-state distribution. Addition of the COOH-terminal 39 residues of rhodopsin redirects the basolateral membrane protein CD7 to the apical membrane. Fusion of rhodopsin's cytoplasmic tail to a cytosolic protein glutathione *S*-transferase (GST) also targets this fusion protein (GST–Rho39Tr) to the apical membrane. The targeting of GST–Rho39Tr requires both the terminal 39 amino acids and the palmitoylation membrane anchor signal provided by the rhodopsin sequence. The apical transport of GST–Rho39Tr can be reversibly blocked at the Golgi complex by low temperature and can be altered by brefeldin A treatment. This indicates that the membrane-associated GST–Rho39Tr protein may be sorted along a yet unidentified pathway that is similar to the secretory pathway in polarized MDCK cells. We conclude that the COOH-terminal tail of rhodopsin contains a novel cytoplasmic apical sorting determinant. This finding further indicates that cytoplasmic sorting machinery may exist in MDCK cells for some apically targeted proteins, analogous to that described for basolaterally targeted proteins.

Key words: MDCK • rhodopsin • apical sorting signal • cytoplasmic amino acids • photoreceptor

Proper sorting/targeting of membrane proteins and lipids is critical in generating and maintaining the plasma membrane asymmetry of polarized neuronal and epithelial cells. Renal epithelial MDCK cells, which form polarized monolayers with distinct apical and basolateral surfaces, provide a useful model for studying vectorial membrane trafficking. Proteins in the secretory pathway are sorted into distinct transport vesicles during transit through the TGN before they are recruited to either the apical or basolateral plasma membrane in MDCK cells (Wandinger-Ness et al., 1990). The fidelity of this intracellular sorting in MDCK cells is very high, suggesting that it is tightly regulated via recognition of specific sorting signals. All basolateral sorting signals described to date reside in the cytoplasmic domain of proteins (for review see Rodriguez-Boulan and Powell, 1992). In contrast, apical targeting motifs have been found to be in the lumenal domain of proteins. For example, cytoplasmic tail–truncated mutants of normally basolateral membrane proteins are targeted to the apical membrane in polarized MDCK cells (Mostov et al., 1986; Hunziker et al., 1991; Prill et al., 1993). Membrane anchor-minus, soluble forms of both apical and basolateral membrane proteins are secreted apically (Mostov et al., 1987; Roth et al., 1987; Lisanti et al., 1989*b*; Prill et al., 1993). Finally, a chimeric protein containing the lumenal domain of apical viral protein hemagglutinin and the transmembrane/cytoplasmic domains of basolateral vesicular stomatitis virus G protein is targeted apically in monkey kidney cells (Roth et al., 1987). Lipid and carbohydrate modifications of proteins also act as apical targeting signals. A glycosyl phosphatidylinositol (GPI)[1] membrane anchor can redirect nonpolar or basolateral proteins to be sorted apically (Brown et al., 1989; Lisanti et al., 1989*b*). The interactions between the GPI-anchored protein and glycosphingolipids in the TGN are thought to result in a clustering of proteins to be sorted together into patches. This process subsequently induces vesicle formation and budding from the TGN membrane

Address all correspondence to Dr. Ching-Hwa Sung, Dyson Vision Research Institute, Cornell University Medical College, 1300 York Avenue, New York, NY 10021. Tel.: (212) 746-2291. Fax: (212) 746-8101. E-mail: chsung@mail.med.cornell.edu

1. *Abbreviations used in this paper*: BFA, brefeldin A; GPI, glycosyl phosphatidylinositol; GST, glutathione *S*-transferase; PFA, paraformaldehyde.

(Simons and Wandinger-Ness, 1990). Both *N*- and *O*-glycans have been suggested to play a role in the apical protein sorting. Removal of *N*-glycans by tunicamycin treatment or site-directed mutagenesis from several apical glycoproteins results in the randomization of sorting (for review see Fiedler and Simons, 1995). Deletion of a region containing O-linked glycosylation signals effectively reverses the sorting of nerve growth factor receptor p75 to the basolateral membrane (Yeaman et al., 1997).

Rhodopsin, a seven-transmembrane G-protein–coupled receptor, is the light absorbing protein in rod photoreceptors. In photoreceptors, rhodopsin is synthesized and processed through the ER–Golgi pathway before it is sorted at the TGN (Schmied and Holtzman, 1989). Post-Golgi rhodopsin-bearing vesicles are then transported vectorially to a specialized, cilium-derived compartment—the outer segment—in which phototransduction occurs. Rhodopsin is targeted to the outer segment with nearly perfect fidelity (Papermaster and Schneider, 1982); more than 90% of rhodopsin is accumulated in this region of photoreceptor at steady state (Sung et al., 1994). Nevertheless, the mechanism underlying the sorting and targeting of rhodopsin in rod cells remains largely unclear. Recently, it has been demonstrated that in a cell-free system, an antibody against rhodopsin's COOH terminus can arrest the exit of newly synthesized rhodopsin-bearing vesicles from the TGN isolated from frog photoreceptors (Deretic et al., 1996), suggesting that this region of protein may be involved in its trafficking. The physiological importance of the COOH-terminal region of rhodopsin is suggested by its highly conserved amino acid sequences among different species and the nonrandom clustering of mutations associated with autosomal dominant retinitis pigmentosa. Retinitis pigmentosa is a hereditary degenerative disease of photoreceptor cells that ultimately leads to blindness. More than a dozen of the known autosomal dominant retinitis pigmentosa mutations are found near the COOH terminus of rhodopsin (for review see Sullivan and Daiger, 1996).

In the present report, we demonstrate that newly synthesized rhodopsin is predominantly delivered directly from the TGN to the apical plasma membrane in MDCK cells. Removal of 32 amino acids from the cytoplasmic tail of rhodopsin results in a randomization of its membrane localization. Moreover, the addition of rhodopsin's cytoplasmic tail can redirect the sorting of other proteins to the apical side of polarized MDCK cells. We propose that the cytoplasmic amino acid sequences of rhodopsin act as an apical sorting signal in MDCK cells.

Materials and Methods

Reagents

DME was purchased from Mediatech (Herndon, VA). Lipofectamine and other cell culture reagents were obtained from Life Technologies (Grand Island, NY). EXPRE^{35}S^{35}S protein labeling mix was purchased from NEN™ Life Science Products (Boston, MA). Protein A–Sepharose was purchased from Pharmacia Biotech (Piscataway, NJ). Affinity-purified rabbit anti–mouse IgG was purchased from Cappell Laboratories (Malvern, PA). Biotin-LC-hydrazide and streptavidin agarose were from Pierce Chemical Co. (Rockville, IL). Anti–γ-adaptin antibody was purchased from Transduction Laboratories (Lexington, KY). Biotinylated secondary antibodies were purchased from Vector Laboratories (Burlingame, CA). FITC-streptavidin was from Amersham Corp. (Arlington Heights, IL). FITC anti–rabbit IgG and Texas red anti–mouse IgG were from Jackson ImmunoResearch Laboratories (West Grove, PA). Brefeldin A (BFA) was purchased from Epicentre Technologies Co. (Madison, WI) and stored frozen as a 5 mg/ml stock in ethanol. PNGase F was purchased from Boehringer-Mannheim Biochemical (Mannheim, Germany). Anti–glutathione *S*-transferase (GST) antibody and all other chemical products were obtained from Sigma Chemical Co. (St. Louis, MO).

Constructs

Rhodopsin mutant constructs used in this report are illustrated in Fig. 1. Stop codons or amino acid changes were introduced into human rhodopsin cDNA by site-directed mutagenesis (Sung et al., 1991) using the oligos 5′-GGCCACCTAGCTCGTCT-3′ (Δ5), 5′-TCACCCAGTTAGTTCTTGCC-3′ (Δ22), 5′-GTGGTGAGCTAGCAGTTCCG-3′ (Δ32), and 5′-AGTGGGTTCTTGCCGGAGGAGATGGTGGTGAGCA-3′ (Cys^{322}Cys^{323} → Ser^{322}Ser^{323}) priming on single-stranded template DNA. In each case, the mutated region was recloned into pCB6, a cytomegalovirus-driven expression vector that had not undergone mutagenesis, and the entire inserted coding region was sequenced.

For the CD7–Rho39 construct, the COOH-terminal 39 amino acids of human rhodopsin (amino acids 310–348) were PCR amplified using the forward primer 5′-CGACCTCGAGAACAAGCAGTTCCGGAACTGCATGC and the reverse primer 5′-ATGCTCTAGAAGTCCTAGGCAGGTCTTAGGC. For the CD7–Rho7 construct, a stop codon was created in the forward PCR primer 5′-CGACCTCGAGAACAAGCAGTTCCGGAACTGCTAGC, and the same reverse primer was used for PCR amplification using wild-type rhodopsin as a template. The PCR products were digested with XhoI/XbaI and inserted into XhoI/XbaI-digested CD7BB plasmid. Plasmid CD7BB is a cytomegalovirus expression vector (pCDM8; Invitrogen, Carlsbad, CA) that contains an XhoI site immediately 3′ to the CD7 coding sequence. The resulting CD7–Rho39 and CD7–Rho7 fusions contain the intact CD7 sequence, two junctional residues (Leu-Glu), and the COOH-terminal sequences of human rhodopsin.

For the GST–Rho39Tr fusion construct, a yeast expression plasmid pDB-Rho39Tr[2] containing the coding sequence of a triple repeat of the terminal 39 residues of rhodopsin was digested with XbaI and NdeI and inserted into XbaI- and NdeI-digested pBC vector. pBC is a eukaryotic GST fusion vector containing an SV-40 enhancer/promoter followed by the open reading frame of GST (Chatton et al., 1995). The resulting fusion contains 50 irrelevant amino acids between the GST and the first rhodopsin sequence and 28 amino acids in between each tandem repeat of the rhodopsin COOH-terminal sequence. In the GST–Rho39pal$^-$Tr construct, the rhodopsin sequences in the GST–Rho39Tr construct were replaced by PCR fragments generated from the Cys^{322}Cys^{323} → Ser^{322}Ser^{323} mutant.

2. Multiple-step constructions were carried out to generate the plasmid pDB-Rho39Tr. First, the coding sequence for rhodopsin's terminal 39 amino acids was PCR amplified from human rhodopsin cDNA (forward: 5′CGGAATTCCGACGAGCATCAGTTGAGAAGCGACGAGCATCAGTTGAGTTCAACAAGCAGTTCCGGAACTGCATGC; reverse: 5′-ATGCTCTAGAAGTCCTAGGCAGGTCTTAGGC), digested with EcoRI/XbaI, and subcloned into EcoRI/XbaI-digested pMAL-cRI (NEB, Beverly, MA) to generate a maltose binding protein–Rho39 fusion construct. The rhodopsin sequence and its flanking restriction sites were then amplified from the maltose binding protein–Rho39 fusion construct (forward: 5′-GGTCGTCAGACTGTCGATGAAGCC; reverse: 5′-AATGTACAGCCGGGGCCACCTGGCTCG), digested with SacI/BsrGI, and ligated into SacI/Acc65I-digested maltose binding protein–Rho39 to generate a maltose binding protein–Rho39Di construct. This procedure was repeated once more to transfer another rhodopsin PCR fragment into SacI/Acc65I-digested maltose binding protein–Rho39Di construct to generate maltose binding protein–Rho39Tr construct. Finally, a PCR fragment containing the coding sequences for a triple repeat of rhodopsin's terminal 39 residues was amplified using maltose binding protein–Rho39Tr as a template (forward: 5′-CATGCCATGGCCAGCGGTCGTCAGACTGTCG; reverse: 5′-GTTGTAAAACGACGGCCAGTGCC) and subcloned into a NcoI/SalI-digested pAS2 vector (CLONTECH Labs, Palo Alto, CA) to obtain pDB-Rho39Tr. All inserts generated by PCR reactions were sequenced to confirm.

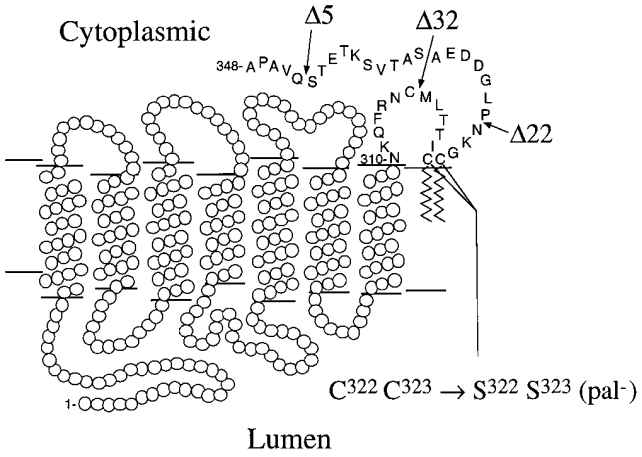

Figure 1. Rhodopsin topology showing COOH-terminal mutant constructs used to characterize the apical sorting domains. Rhodopsin is a seven-transmembrane protein with its COOH terminus facing the cytoplasmic side and its NH_2 terminus facing the extracellular side of the lipid membrane. The zigzags indicate the palmitoyl membrane anchor sites. All mutants used in this study were generated using site-directed in vitro mutagenesis. Δ5, Δ22, and Δ32 are COOH-terminal deletion mutants in which the last 5, 22, and 32 amino acid residues are missing, respectively. In the $Cys^{322}Cys^{323} \rightarrow Ser^{322}Ser^{323}$ (pal^-) mutant, the cysteines at positions 322 and 323 were replaced with serines. The residues between amino acids 310 and 348 are labeled with single-letter amino acid designations.

Cell Culture and Transfection

MDCK cells (type II) were maintained in DME supplemented with 5% fetal bovine serum, penicillin (50 U/ml), and streptomycin (50 μg/ml). Transfection of MDCK cells was performed using lipofection following the manufacturer's instructions. Stable cell lines were obtained by G418 (500 μg/ml) selection, and positive clones were screened by immunofluorescent staining. MDCK stable transfectants were seeded at high density (1.5×10^6 cells/24-mm filter or equivalent density) in Costar™ (Cambridge, MA) polyester clear Transwells for 5–7 d to allow the development of a tight monolayer. For each construct, at least two independent clonal lines were selected and used for the experiments.

In the temperature blocking experiments, MDCK cultures were incubated at 20°C for the indicated time followed by immunofluorescent labeling as described below. To release the proteins blocked in the TGN during the low-temperature incubation, the cells were shifted back from 20°C block to 37°C for different periods of time as indicated in the text. 20 μg/ml of cycloheximide was added to the culture at the beginning of the 37°C incubation to suppress protein synthesis.

Immunofluorescent Staining

For surface immunofluorescent staining, filter-grown MDCK monolayers were washed with ice-cold phosphate buffered saline containing 2 mM $MgCl_2$ and 0.2 mM $CaCl_2$ (PBS-C/M) and incubated with mAb B6-30 (antirhodopsin NH_2 terminus) (Adamus et al., 1988) or T3-3A1 (anti-CD7 NH_2 terminus; American Type Culture Collection, Rockville, MD) from both sides for 30 min at 4°C. After extensive washing with cold PBS-C/M, cells were fixed with 2% paraformaldehyde (PFA) for 30 min, quenched with 50 mM ammonium chloride for 10 min, rinsed, and then incubated with biotinylated goat anti–mouse antibody (1:200) and FITC-streptavidin (1:25).

For temperature shift experiments, cells were immediately washed with ice-cold PBS-C/M and fixed with 2% PFA after different incubation conditions. Fixed cells were quenched and then permeabilized with 0.075% saponin, 0.5% BSA in PBS-C/M for 30 min. Permeabilized cells were incubated with primary antibody (1:1,000 for anti-GST antibody; 1:100 for anti–γ-adaptin antibody) for 1 h followed by fluorophore-conjugated secondary antibodies (1:50) in permeabilization buffer for an additional 1 h. In some experiments, biotinylated anti–rabbit antibody (1:200) followed by FITC-streptavidin was used to visualize GST proteins. For nuclear staining, cells were treated with DNase-free RNase (1:100; 5 prime → 3 Prime, Boulder, CO) during secondary antibody incubation and then incubated with propidium iodide (10 μg/ml) for an additional 15 min. The immunostaining was examined using a laser scanning confocal microscope (Molecular Dynamics, Sunnyvale, CA).

Domain Selective Biotinylation/Membrane Targeting Assay

To quantitate the steady-state protein distribution on the apical and basolateral sides of MDCK cells, a domain-selective biotinylation/immunoprecipitation assay was performed as described (Lisanti et al., 1989*a*). In brief, filter-grown MDCK cells expressing rhodopsin were surface labeled either apically or basolaterally using biotin-LC-hydrazide. Membrane-impermeant biotin-LC-hydrazide biotinylates the carbohydrate located at the extracellular domains of rhodopsin or CD7. After biotinylation, the filters were washed with cold PBS-C/M and excised. Cells were then solubilized in lysis buffer (1% Triton X-100, 50 mM Tris, pH 7.5, 150 mM NaCl, and 2 mM EDTA) containing protease inhibitor cocktail (1 μm PMSF, 2 μg/ml aprotinin, 2 μg/ml leupeptin, and 0.7 μg/ml pepstatin) at 4°C for 1 h, and the cell lysates were centrifuged at 13,000 rpm for 20 min. Our preliminary results have shown that rhodopsin was almost completely solubilized in Triton X-100 under these extraction conditions. The supernatant was immunoprecipitated with protein A–Sepharose precoated with rabbit anti–mouse antibody plus mAb B6-30 or mAb T3-3A1. The eluted immunocomplexes were electrophoresed on SDS-PAGE, transferred to nitrocellulose, and blotted with ^{125}I-streptavidin (Amersham Corp.) as described. Quantitation of biotinylated rhodopsin recovered from the apical and basolateral domains was determined by a PhosphorImager (Molecular Dynamics).

A membrane targeting assay (Le Bivic et al., 1989) was carried out to follow the delivery of newly synthesized rhodopsin to the membrane. MDCK monolayers expressing rhodopsin were pulse labeled with EXPRE^{35}S^{35}S protein labeling mix from the basolateral side for 20 min. At varying time points during the chase, cells were chilled to 4°C and biotinylated from the apical or basolateral surface using biotin-LC-hydrazide. After biotinylation, cells were lysed and immunoprecipitated as described above. The immunoprecipitates were dissociated from the Sepharose beads by boiling the samples in 40 μl 5% SDS for 5 min and then diluting them with 460 μl of lysis buffer. A 50-μl fraction was directly analyzed on SDS-PAGE to demonstrate that equal amounts of radiolabeled protein were precipitated from each sample. The remainder of the samples was subsequently reprecipitated with immobilized streptavidin agarose. This immunoprecipitate was separated by SDS-PAGE and visualized by fluorography. Fractions of biotinylated, radiolabeled immunoprecipitates were digested by PNGase F as described (Sung et al., 1991) followed by SDS-PAGE analysis.

Subcellular Fractionation

Fractionation of cytosol (S100) and total membrane (P100) was carried out according to a protocol described previously (van't Hof and Resh, 1997) with minor modifications. In brief, cells were washed and scraped from Transwell filters in ice-cold buffer (50 mM Tris, pH 7.5, 150 mM NaCl, and 2 mM EDTA) and spun for 5 min at 2,000 rpm. Cells were resuspended in isotonic buffer (10 mM Tris, pH 7.2, 0.2 mM $MgCl_2$, 250 mM sucrose, 1 mM EDTA, plus protease inhibitors), sheared by 22-gauge needles, and homogenized with a Balch homogenizer (Balch et al., 1984). Postnuclear supernatants, prepared by spinning the cell homogenates at 3,000 *g* for 10 min, were then centrifuged for 45 min at 100,000 *g* (model TLA 100.3 rotor; Beckman Instruments, Fullerton, CA). The resulting supernatant (S100) was supplemented with 0.2 vol of 5× concentrated lysis buffer, and the pellet (P100) was resuspended in an equal volume of 1× lysis buffer (50 mM Tris, pH 8.0, 150 mM NaCl, 2 mM EDTA, 1% NP-40, 0.5% deoxycholate, plus protease inhibitors). Samples were then lysed on ice for 15 min and cleared by centrifugation at 100,000 *g* for 15 min. Equal volumes of P100 and S100 were subjected to SDS-PAGE followed by immunoblotting analysis.

Results

Rhodopsin's COOH Terminus Is Necessary for Its Apical Sorting in MDCK Cells

The membrane distribution of native rhodopsin in polar-

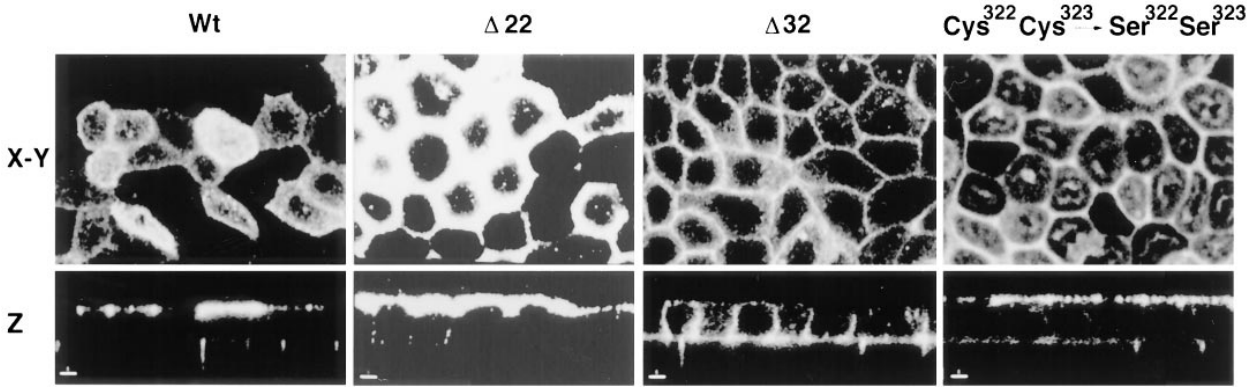

Figure 2. Immunolocalization of wild-type (*Wt*) and mutant rhodopsins in stably transfected MDCK cells. Rhodopsin was detected by surface immunofluorescent labeling using mAb B6-30 as described in Materials and Methods. The immunofluorescent staining was analyzed by laser scanning confocal microscopy. Optical sections horizontal (*X-Y*, *top*) and perpendicular (*Z*, *bottom*) to the monolayer are shown. Note that the clear Transwell filter itself generates a weak background. Bar, 5 μm.

ized MDCK cells was first determined by surface immunofluorescent staining. Monolayers of MDCK cells stably expressing rhodopsin were incubated from both sides with mAb B6-30, which recognizes the extracellular NH_2 terminus of rhodopsin at 4°C for 30 min. The cells were then washed and fixed, and rhodopsin was visualized by incubating with biotinylated anti–mouse IgG followed by FITC-conjugated streptavidin. En face images of confocal microscopic analysis revealed a characteristic tile-like, apical labeling of rhodopsin (Fig. 2, *top panel*). The vertical scan confirmed that rhodopsin is almost exclusively localized on the apical membrane (Fig. 2, *bottom panel*).

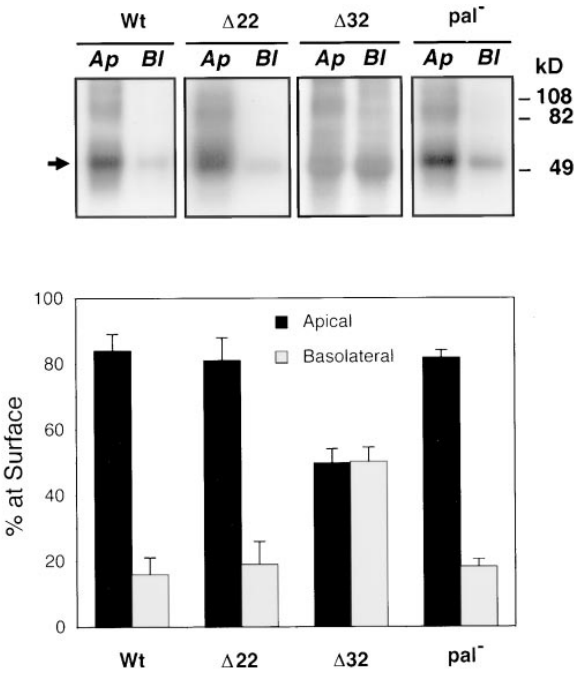

Figure 3. The steady-state surface distribution of rhodopsins expressed in stably transfected MDCK cells. The immunoprecipitated, biotinylated rhodopsin proteins were electrophoresed on 12% SDS-PAGE, transferred to a nitrocellulose filter, and probed with ^{125}I-streptavidin as described in Materials and Methods. Note that rhodopsin is prone to forming higher-order aggregates (Sung et al., 1991). The arrow indicates the monomeric form. Blots were analyzed with a Molecular Dynamics PhosphorImager. The total rhodopsin expressed on the cell surface was taken to be 100%. Bars represent the mean ± SD of multiple determinations from more than three independent experiments (n = 5, 5, 6, and 4 for Wt, Δ22, Δ32, and pal$^-$, respectively). Signals derived from multimers were also taken into consideration in quantitation. pal$^-$ = $Cys^{322}Cys^{323} \rightarrow Ser^{322}Ser^{323}$ mutant.

To confirm and quantify the steady-state distribution of rhodopsin, we used a domain-selective biotinylation/immunoprecipitation assay in which MDCK monolayers were selectively biotinylated from either surface. The cell lysates were immunoprecipitated by mAb B6-30, electrophoresed, and transferred onto nitrocellulose membrane. The biotinylated rhodopsin was then detected and quantified by the amount of bound ^{125}I-streptavidin. In agreement with the immunofluorescent labeling, the majority of the wild-type rhodopsin (~84%) was found to be expressed apically (Fig. 3).

To test whether the cytoplasmic tail of rhodopsin contains apical sorting information, a nested set of COOH-terminal deleted mutant rhodopsins was constructed, and these rhodopsins were stably expressed in MDCK cells (Fig. 1). Using both surface immunofluorescent labeling (Fig. 2) and the domain-selective biotinylation/immunoprecipitation assay (Fig. 3), we found that a deletion of the terminal five residues (Δ5, ~80% apical, data not shown) or 22 residues (Δ22, ~81% apical) did not affect the apical sorting pattern of rhodopsin. However, a deletion of 32 amino acids resulted in the loss of apical polarity, with the truncated mutant rhodopsin (Δ32) expressed on both the apical and basolateral surfaces at similar levels. These results suggest that the terminal 32 residues of rhodopsin's cytoplasmic tail contain the necessary information required for its apical targeting.

Palmitoylation Is Not Required for the Apical Targeting of Rhodopsin

Fatty acylation, such as palmitoylation, is a feature of several membrane-associated proteins, including neuromodulin (Zuber et al., 1989), the Src family of protein tyrosine kinases (Shenoy-Scaria et al., 1994), vaccinia viral protein (Grosenbach et al., 1997), and heterotrimeric G proteins

(Wedegaertner et al., 1995). Fatty acylation not only provides membrane anchoring for these otherwise cytosolic proteins but also mediates their proper cellular targeting (Liu et al., 1994; Shenoy-Scaria et al., 1994; Garcia-Cardena et al., 1996). Two highly conserved cysteine residues, Cys^{322} and Cys^{323}, located in the cytoplasmic tail of rhodopsin, are known to be palmitoylated and membrane anchored (Applebury and Hargrave, 1986; Papac et al., 1992). So far, no signal transduction function has been assigned to this palmitoyl modification of rhodopsin (Karnik et al., 1988; Osawa and Weiss, 1994). These palmitoylation signals are deleted in the Δ32 mutant rhodopsin, as described above, which has altered domain expression in MDCK cells. We therefore examined whether the palmitoyl moiety of rhodopsin plays a role in its sorting. A nonpalmitoylated, site-directed mutant rhodopsin $Cys^{322}Cys^{323} \rightarrow Ser^{322}Ser^{323}$ (Fig. 1, Karnik et al., 1988) was stably transfected into MDCK cells, and its expression was examined by both immunostaining (Fig. 2) and domain-selective membrane targeting assay (Fig. 3). We concluded that the $Cys^{322}Cys^{323} \rightarrow Ser^{322}Ser^{323}$ mutant exhibits apical expression in MDCK cells (~82% apical), indistinguishable from the wild-type rhodopsin. This result suggests that neither the $Cys^{322}Cys^{323}$ residues nor their resulting palmitoylation is essential for rhodopsin's apical sorting.

Rhodopsin's COOH Terminus Is Sufficient to Redirect CD7 to the Apical Surface of MDCK Cells

To address whether the cytoplasmic tail of rhodopsin is sufficient for apical sorting, a single transmembrane domain protein CD7 was chosen as a reporter protein. CD7 has been reported to be a "bulk-flow" membrane marker in MDCK cells and appears on both the apical and the basolateral surfaces in a nonpolar manner (Haller and Alper, 1993). Nevertheless, to our surprise, in three independent MDCK stable clones we examined, CD7 was detected basolaterally (~82%) in the biotinylation/immunoprecipitation assay (Fig. 4 *C*). Indirect immunofluorescence and laser scanning confocal microscopy of cells stained with antibodies against CD7 showed that immunofluorescent CD7 signal was observed predominantly on the basolateral surface, although some of the signal can also be detected on the apical surface at variable levels (Fig. 4 *B*). We later confirmed that CD7 is primarily sorted to the basolateral surface of MDCK cells through a direct pathway from the TGN (see below). Similar results were also observed by another group (Chen, Y.-T., personal communication). This discrepancy regarding the targeting of CD7 likely reflects variability in the sorting patterns of MDCK sublines. This phenomenon has also been observed for other proteins (Ojakian et al., 1987; Mays et al., 1995). In contrast to CD7, we found that the fusion protein CD7–Rho39, produced by fusion of the entire rhodopsin's cytoplasmic tail 39 amino acids to the COOH terminus of CD7 (Fig. 4 *A*), was apically sorted in MDCK cells assayed by surface immunofluorescent labeling using anti-CD7 antibody (Fig. 4 *B*). Identical staining of CD7–Rho39 was observed upon immunolabeling permeabilized cells with mAb 1D4, an antibody which recognizes the COOH ter-

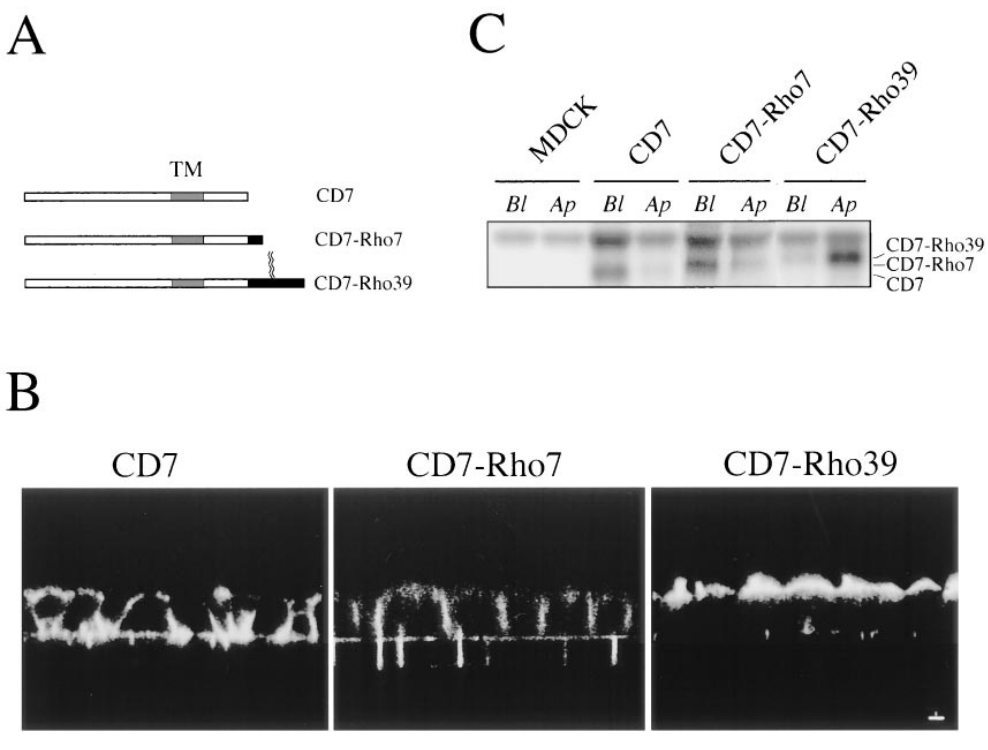

Figure 4. Apical targeting of CD7 by rhodopsin's COOH terminus. (*A*) Schematic diagrams of CD7, CD7–Rho7, and CD7–Rho39. CD7–Rho7 is a fusion protein in which the proximal seven residues of rhodopsin's cytoplasmic tail (N^{310}-C^{316}) is fused to the COOH terminus of CD7 (*open box*). CD7–Rho39 is a CD7 fusion protein containing rhodopsin's COOH-terminal 39 residues (N^{310}-A^{348}). *TM*, transmembrane domain; *zigzag*, palmitoyl membrane anchor; *black box*, rhodopsin sequence. (*B*) Polarized MDCK monolayers stably expressing CD7, CD7–Rho7, and CD7–Rho39 after surface immunofluorescent labeling with mAb T3-3A1, which recognizes the extracellular domain of CD7. Vertical optical sections obtained from confocal microscopic analysis are shown. (*C*) The levels of steady-state surface distribution of CD7 (~40 kD), CD7–Rho7 (~41 kD), and CD7–Rho39 (~44 kD) were determined by the domain-selective biotinylation/immunoprecipitation assay. As was shown previously (Haller and Alper, 1993), an endogenous MDCK protein that migrates slightly slower than CD7–Rho7 and CD7–Rho39 on SDS-PAGE is also precipitated by mAb T3-3A1. Results shown are from a representative experiment chosen between four trials using more than two independent stable lines. Bar, 5 μm.

minus of rhodopsin (Hodges et al., 1988) (data not shown). Little or no specific basolateral staining was detected in these cells. In agreement with the immunostaining results, ~89% of CD7–Rho39 fusion proteins were detected on the apical surface biochemically (Fig. 4 *C*). The apical localization of the CD7–Rho39 fusion demonstrates that rhodopsin's COOH-terminal sequence is able to provide sufficient apical-sorting information to function independently on another membrane protein.

To test whether the palmitoylation is involved in the apical targeting of CD7–Rho39, the surface distribution of palmitoylation-negative CD7–Rho39pal$^-$ in MDCK stable lines was examined immunochemically and biochemically. We found that CD7–Rho39pal$^-$ was sorted predominantly to the apical surface (~72% at steady state, data not shown). This finding reinforces the notion that the palmitoylation may not play a critical role in the apical targeting activity.

To demonstrate that the apical targeting of CD7–Rho39 was due to the rhodopsin sequences rather than inactivation of a putative basolateral targeting signal of CD7, we examined the distribution of CD7–Rho7 (a truncated form of CD7–Rho39 in which the distal 32 residues of rhodopsin's cytoplasmic tail were deleted [Fig. 4 *A*]) in MDCK cells. The immunofluorescent staining pattern of CD7–Rho7 was indistinguishable from that of CD7 itself (Fig. 4 *B*). The membrane targeting assay suggested that, at steady state, CD7–Rho7 was predominantly sorted basolaterally (~74% basolateral, Fig. 4 *C*). This result argues that the addition of extra nonspecific sequences to CD7's COOH terminus has little or no effect on its membrane localization. Therefore, the apical transport of CD7–Rho39 is due to the positive apical sorting signal conveyed by the rhodopsin sequences rather than to masking of any putative CD7 COOH-terminal basolateral sorting signal. Moreover, this result further supports the previous data showing that the last 32 residues of rhodopsin contain critical information for the apical sorting activity.

Rhodopsin and CD7–Rho39 Are Directly Targeted from the TGN to the Apical Surface

To investigate the intracellular routing of wild-type rhodopsin in MDCK cells, we traced the cell surface delivery of newly synthesized rhodopsin using a pulse-chase/membrane targeting assay. Confluent MDCK monolayers were pulse labeled with [^{35}S]methionine/cysteine, chased for different times, biotinylated from either the apical or basolateral surface, lysed, and immunoprecipitated by mAb B6-30. The precipitated rhodopsin molecules were subsequently precipitated by streptavidin-agarose, so that only the radiolabeled rhodopsin that had reached the cell surface by the time of biotinylation was detected by autoradiography. After 30 min of chase, no rhodopsin was detected on either surface (Fig. 5 *B*). At this time point, we found that the majority of the newly synthesized rhodopsin was in an immature, endo H–sensitive (data not shown) glycosylated form, which migrates slightly faster than the mature form (Fig. 5 *A*). After 1 h of chase, rhodopsin began to appear on the apical surface as indicated by a smear of bands on SDS-PAGE analysis (Fig. 5 *B*). This appearance is typical for proteins that have undergone heterogeneous Golgi sugar processing. In this state, they are characterized by their resistance to endo H cleavage (Sung et al., 1991; data not shown). These smear bands can be trimmed to a core polypeptide of ~38 kD by treating the immunoprecipitates with PNGase F (Fig. 5 *C*). It is evident that newly synthesized rhodopsin was delivered predominantly to the apical plasma membrane at all time points tested, suggesting that rhodopsin follows a direct route from the TGN to the apical membrane.

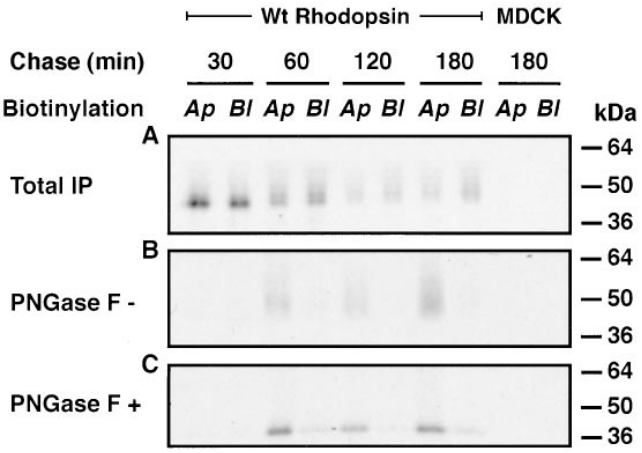

Figure 5. Targeting of wild-type rhodopsin from TGN to the apical surface. Vectorial delivery of wild-type rhodopsin to the cell surface was analyzed by a membrane targeting assay (see Materials and Methods). At various time points during the chase as indicated, ^{35}S metabolically labeled, rhodopsin-expressing MDCK cells were biotinylated from either the apical (*Ap*) or basolateral (*Bl*) surface and immunoprecipitated with antirhodopsin mAb B6-30 as described. (*A*) A fraction of each immunoprecipitated sample was analyzed by 4–20% SDS-PAGE and is shown as total immunoprecipitate. (*B*) Biotinylated, radiolabeled immunoprecipitates were obtained by a subsequent reprecipitation with streptavidin agarose. (*C*) For quantitation, biotinylated, radiolabeled immunoprecipitates were treated with PNGase F, separated by SDS-PAGE, and visualized by autoradiography. No labeled material is precipitated from control MDCK cell lysates.

The intracellular transport of CD7–Rho39 fusion protein was also examined using the same membrane targeting assays. We found that after 30 min, 1 h, and 2 h of chase, ~65, 75, and 78%, respectively, of CD7–Rho39 fusion proteins were detected on the apical surface (Fig. 6 *A*), whereas CD7 alone was predominantly targeted to the basolateral side at all chase time points tested (Fig. 6 *C*). In both cases, equal amounts of total radiolabeled protein were immunoprecipitated from each sample (Fig. 6, *B* and *D*). These results are consistent with the steady-state surface distribution of these two proteins. The direct apical targeting of CD7–Rho39 fusion protein suggests that similar mechanisms may be used for the sorting/targeting of both CD7–Rho39 and wild-type rhodopsin in MDCK cells.

The Palmitoylated Rhodopsin Cytoplasmic Tail Enables a Cytosolic Protein to Be Delivered to the Apical Surface

To confirm that there is no recessive information present

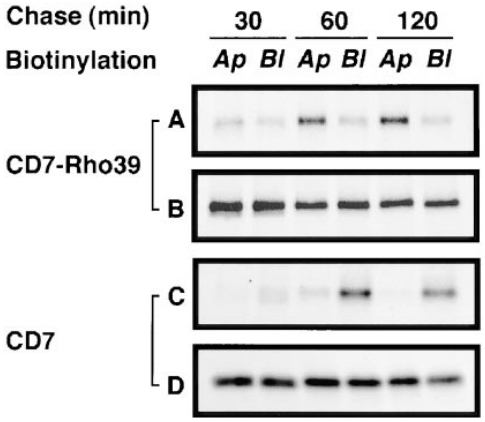

Figure 6. Targeting of CD7–Rho39 directly from the TGN to the apical surface. Targeting of CD7–Rho39 and CD7 was analyzed by the membrane targeting assay described in Fig. 5. In this experiment, the CD7–Rho39 fusion protein was precipitated by antirhodopsin COOH terminus mAb 1D4, and CD7 was precipitated by anti-CD7 mAb T3-3A1. (*A* and *C*) Autoradiograms of biotinylated, radiolabeled immunoprecipitates, which were analyzed by 12% SDS-PAGE. (*B* and *D*) Before the second streptavidin-agarose precipitation, fractions of total radiolabeled 1D4 or T3-3A1 immunoprecipitates were analyzed on SDS-PAGE to demonstrate that equal amounts of radiolabeled proteins were immunoprecipitated from each sample. *Ap*, apically biotinylated; *Bl*, basolaterally biotinylated.

in the lumenal or transmembrane domains of rhodopsin or CD7, which is necessary for the apical targeting activity, we tested whether the cytoplasmic tail of rhodopsin can be recognized in the absence of any transmembrane or lumenal domains. We made a fusion protein GST–Rho39Tr, in which the cytosolic protein GST was fused to a triple-repeat of the COOH-terminal 39 residues of rhodopsin (Fig. 7 *A*). A triple repeat was chosen because the placement of the putative signal at varying distances from GST minimizes any steric hindrance of the signal by GST. We reasoned that the GST–Rho39Tr would likely be membrane anchored via the palmitoylation signal provided by the rhodopsin sequences. A nonpalmitoylated GST fusion (GST–Rho39pal$^-$Tr) was also generated by replacing the wild-type rhodopsin sequence with the $Cys^{322}Cys^{323} \rightarrow Ser^{322}Ser^{323}$ mutant sequence for comparison (Fig. 7 *A*). MDCK cells stably expressing control GST protein, GST–Rho39Tr, or GST–Rho39pal$^-$Tr were PFA fixed, permeabilized, and immunolabeled with anti-GST antibody. GST–Rho39Tr protein in MDCK cells grown on coverslips was found to be primarily associated with the plasma membrane (see below). In filter-grown polarized cells, we found that the GST–Rho39Tr fusion protein was detected almost exclusively on the apical plasma membrane (Fig. 7 *B*, *middle*). Likewise, the subcellular fractionation assay showed that the GST–Rho39Tr fusion protein was predominantly localized in the membrane fraction (P100)

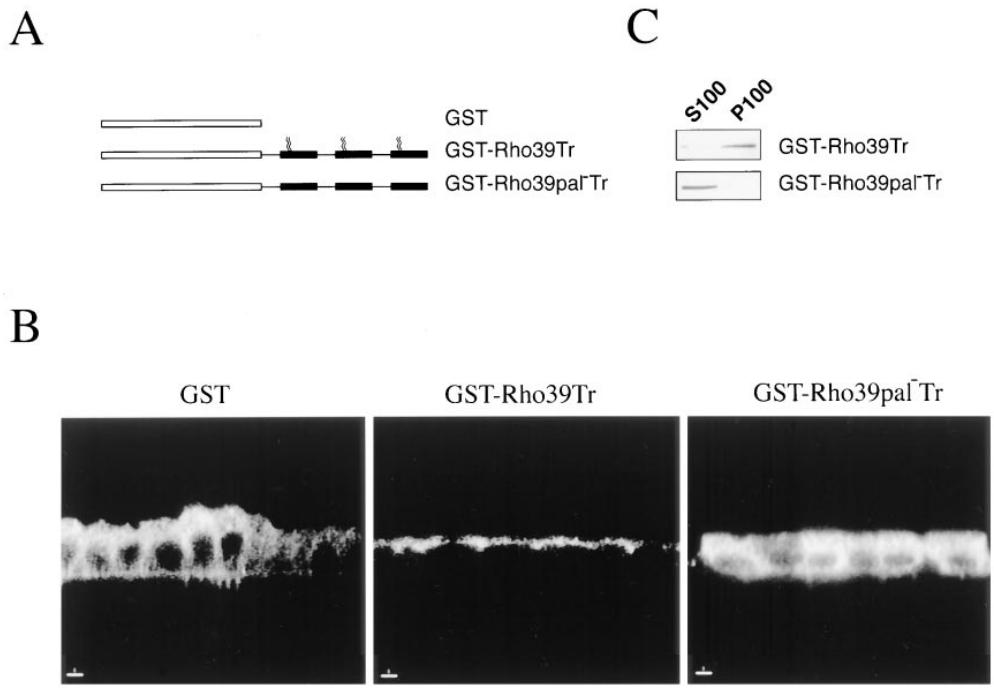

Figure 7. The apical targeting of GST by addition of rhodopsin's COOH terminus. (*A*) Schematic diagrams of GST, GST–Rho39Tr, and GST–Rho39pal$^-$Tr. GST–Rho39Tr is a fusion protein in which a triple-repeat of the terminal 39 amino acids of rhodopsin (*black boxes*) was fused to the COOH terminus of GST (*open box*). GST–Rho39pal$^-$Tr is a similar fusion protein except that the 39 rhodopsin residues were derived from the $Cys^{322}Cys^{323} \rightarrow Ser^{322}Ser^{323}$ mutant so that the palmitoylation signal (*zigzag*) was removed. (*B*) Immunolocalization of GST, GST–Rho39Tr, and GST–Rho39pal$^-$Tr in MDCK cells. Permeabilized MDCK monolayers were labeled with anti-GST antibody followed by biotinylated anti–rabbit antibody and FITC-streptavidin. Optical sections perpendicular to the monolayer are shown. Both GST and GST–Rho39pal$^-$Tr show diffuse, nucleus-excluded cytoplasmic staining. (*C*) Subcellular distributions of GST–Rho39Tr and GST–Rho39pal$^-$Tr in MDCK cells. MDCK cell homogenates were fractionated into cytosolic (*S100*) and total cellular membrane (*P100*) fractions by centrifugation at 100,000 *g* for 45 min. Equal fractions of S100 and P100 were electrophoresed on SDS-PAGE and immunoblotted with mAb 1D4 followed by alkaline phosphatase anti–mouse IgG. NBT/BCIP substrates were used for color development. Bar, 5 μm.

(Fig. 7 *C*). More recently, we found that a single repeat of rhodopsin's cytoplasmic tail containing the GST fusion protein is also targeted to the apical plasma membrane in polarized MDCK cells (data not shown). Conversely, the GST–Rho39pal$^-$Tr protein was associated with the cytosolic (S100) fraction (Fig. 7 *C*) and exhibited a uniform, diffuse cytoplasmic staining (Fig. 7 *B*, *right*). This staining was indistinguishable from that of the control GST protein (Fig. 7 *B*, *left*). Since neither the cysteine residues nor the palmitoylation signal is essential for rhodopsin's transport, we predict that the palmitoylation itself of GST–Rho39Tr does not encode specific apical targeting information (see Discussion). However, this result suggests to us that recognition of the apical sorting signal contained in the rhodopsin terminal 39 residues requires membrane anchorage, which can be provided by palmitoylation and/or transmembrane domains.

Little is known about how membrane-associated proteins are targeted to their destined membrane domains. How is the GST–Rho39Tr fusion protein, presumably synthesized by free ribosomes, targeted to the apical plasma membrane: is GST–Rho39Tr recognized and sorted by the similar pathway used for rhodopsin? Or is GST–Rho39Tr directly targeted to the apical membrane from the site of synthesis? We have noted that in subconfluent MDCK cultures, GST–Rho39Tr protein can be detected in a perinuclear, Golgi-like distribution in addition to the plasma membrane (Fig. 8, *a* and *b*). Subcellular membrane fractionation also revealed that GST–Rho39Tr was concentrated in the fractions containing the peak activities of α-mannosidase II and alkaline phosphatase, markers for Golgi and plasma membrane, respectively (data not shown). To gain further insight into the possible transport pathway of GST–Rho39Tr, we studied the effect of a 20°C temperature block on the distribution of GST–Rho39Tr. This low-temperature block is known to inhibit the classical secretory pathway by preventing secreted proteins from exiting the Golgi apparatus (Matlin and Simons, 1983). The distribution of GST–Rho39Tr protein in low temperature–blocked MDCK cells was examined by immunofluorescent staining. In the first part of our analyses, we used subconfluent cells grown on coverslips for optimum resolution of detection of the fluorescent markers. We found that upon 20°C incubation, GST–Rho39Tr accumulated quantitatively in a Golgi-like distribution, which largely overlapped with the TGN marker γ-adaptin (Fig. 8, *c* and *d*). A 2-h 20°C block was effective, whereas a prolonged low-temperature block (6–14 h) not only increased the GST–Rho39Tr levels in the TGN but also gradually depleted the GST–Rho39Tr plasma membrane population. In contrast, this low-temperature incubation had no effect on the diffuse, cytoplasmic staining of GST–Rho39pal$^-$Tr (data not shown), indicating that the Golgi localization of the GST–Rho39Tr fusion protein is dependent on palmitoylation.

We then examined the effect of 20°C incubation in polarized MDCK monolayers and tested whether the surface transport of GST–Rho39Tr could be resumed by shifting cells back to 37°C. MDCK monolayers expressing GST–Rho39Tr were incubated at 20°C for 6 h and then transferred to medium containing cycloheximide and incubated at 37°C for different periods of time before the cells were fixed, permeabilized, and immunolabeled. After the low-temperature block, GST–Rho39Tr was found to be pre-

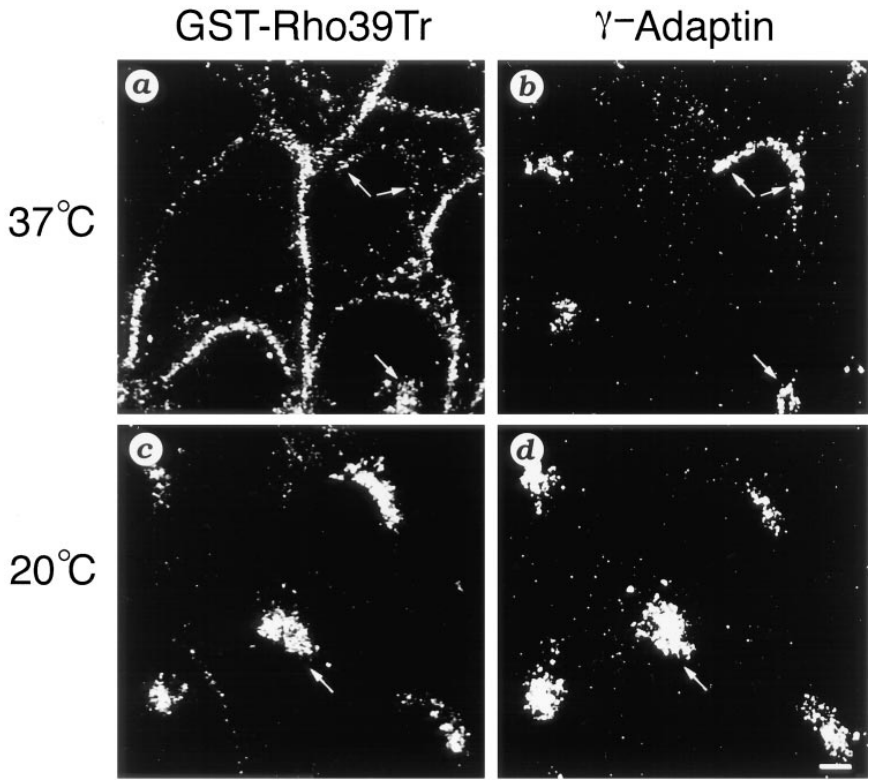

Figure 8. TGN accumulation of GST–Rho39Tr in MDCK cells during a low-temperature block. MDCK cultures grown on coverslips were maintained either at 37°C (*a* and *b*) or removed to 20°C for 6 h (*c* and *d*) before PFA fixation. Fixed cells were permeabilized and double-labeled with anti-GST antibody (*a* and *c*) and anti–γ-adaptin antibody (*b* and *d*). Corresponding fluorescent-conjugated secondary antibodies were used for visualization. Confocal images of the *xy* plane are shown. Arrows indicate the perinuclear, Golgi-like staining. Bar, 5 μm.

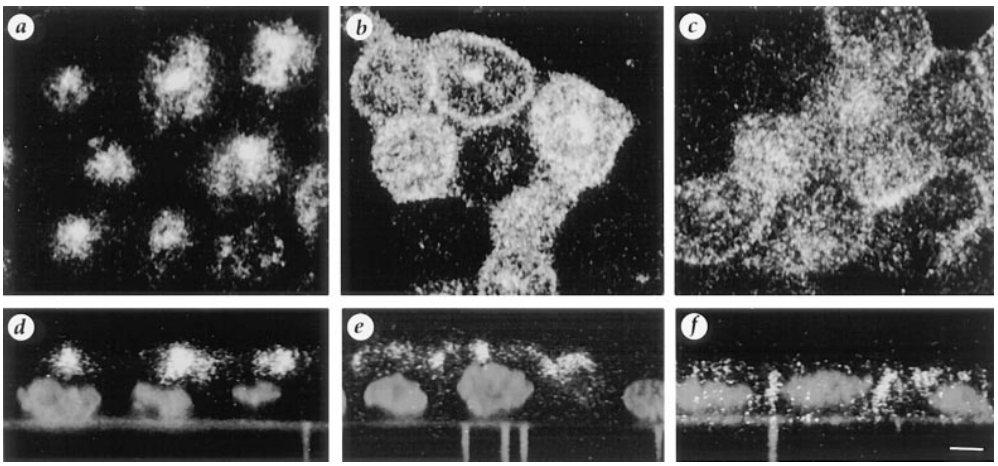

Figure 9. Return of the apical surface localization of GST–Rho39Tr after release from low-temperature block. Monolayers of MDCK cells were incubated at 20°C for 6 h to accumulate newly synthesized GST–Rho39Tr in the Golgi complex. Cells were either immediately fixed by PFA (*a* and *d*) or transferred to medium containing cycloheximide (20 μg/ml) (*b* and *e*) for an additional 30 min at 37°C before fixation. For BFA treatment experiments, 1 μg/ml BFA was added to the cells in the last 15 min of the 20°C incubation and remained during the 37°C release (*c* and *f*). Fixed cells were permeabilized and then immunolabeled with anti-GST antibody, biotinylated anti–rabbit IgG, and streptavidin-FITC. Propidium iodide was included in the staining to show the nuclei in the *z* section (shown in *gray* in *d–f*). After the 20°C block, GST–Rho39Tr is concentrated in the Golgi complex, which is localized above the nucleus in the subapical membrane cytoplasm (*d*). Prominent labeling of GST–Rho39Tr is readily detectable on the apical surface 30 min after 37°C release in control cells (*b* and *e*). However, GST–Rho39Tr accumulates on the basolateral membrane as well as the apical membrane in the cells treated with BFA. Some punctate, intracellular staining of GST–Rho39Tr is also observed (*c* and *f*). The focal plane of *c* was set near the apical surface. Confocal images of both *xy* (*top row*) and *z* (*bottom row*) planes are shown. Bar, 5 μm.

dominantly concentrated in a region above the nucleus and in close proximity to the apical membrane (Fig. 9, *a* and *d*), where the Golgi complex is located in polarized MDCK cells (Bacallao et al., 1989). This GST–Rho39Tr localization appears quite distinct from the fluid-phase marker labeled endosomal compartments (Bomsel et al., 1989). Viewed in the z-plane by confocal microscopy, only low residual levels of GST–Rho39Tr could be detected on the apical surface after this prolonged temperature block. Because there is little or no decrease of surface GST–Rho39Tr during a short 20°C incubation, the significant increase of GST–Rho39Tr at the Golgi complex is unlikely to be the result of recycling from the apical surface (data not shown). Within 30 min of the 37°C release, the majority of GST–Rho39Tr labeling has moved onto the apical surface. This increasing apical GST–Rho39Tr labeling is accompanied by a decreasing Golgi-like, GST–Rho39Tr labeling (Fig. 9, *b* and *e*). The intensity of apical surface labeling of GST–Rho39Tr peaks at 1 h release and is not noticeably increased after 1 h (data not shown). This fast release occurred in the presence of cycloheximide, indicating that the rapidly released GST–Rho39Tr proteins detected on the apical surface had just exited from the Golgi apparatus and were not newly synthesized.

BFA is a fungal metabolite known to effectively block ER–Golgi surface secretion of various proteins in several cell lines. In MDCK cells, low concentrations of BFA (1 μg/ml) have been shown to alter the TGN to surface transport of apical membrane protein dipeptidyl peptidase IV (Low et al., 1992). To assess the effect of BFA on the surface transport of GST–Rho39Tr, MDCK monolayers were treated with BFA during the last 15 min of the low-temperature block and during the 37°C incubation. We found that GST–Rho39Tr protein was distributed to both apical and basolateral membranes in an apparently nonpolar fashion in the presence of BFA (Fig. 9, *c* and *f*). Some bright, punctate staining of GST–Rho39Tr was also found to be distributed throughout the cytoplasm in the cells treated with BFA. The alteration of the apical distribution of GST–Rho39Tr by BFA is similar to the behavior of other apically secreted proteins (Low et al., 1992; Arreaza and Brown, 1995). The effects of low-temperature block and BFA treatment both support the possibility that the apical transport pathway of GST–Rho39Tr shares common mechanisms with the classic secretory pathway in polarized epithelial cells.

Discussion

In the present report, we demonstrate that wild-type rhodopsin is predominantly targeted to the apical surface in polarized MDCK cells. Removal of the terminal 32 amino acids from the cytoplasmic tail of rhodopsin abolished this vectorial targeting. The truncated protein was sent to both the apical and the basolateral membranes at roughly equivalent levels, presumably because of the lack of any sorting information. To confirm that the sorting determinants are present in the cytoplasmic tail of rhodopsin, we show that the COOH-terminal 39 residues of rhodopsin can redirect apical targeting of two heterologous proteins, CD7 and GST. The result of the CD7–Rho7 experiment suggests that additional irrelevant sequences fused to the CD7's COOH terminus are unable to alter its membrane localization, indicating that the apical sorting of CD7–Rho39 is caused by a bona fide sorting activity provided by rhodopsin's sequences. Another reporter protein used in this report is the cytosolic GST protein, which presumably contains no sorting signal. To our knowledge, this is the first time that sorting of an apical protein was found to be mediated by cytoplasmic amino acids.

Possible Mechanisms of Apical Targeting of Rhodopsin

We surmise that the mechanism for the sorting of rhodopsin must be distinct from that used for the recognition of previously described apical sorting signals, such as lumenal ectodomains, GPI anchors, or glycans. We have found no significant homology between the COOH terminus of rhodopsin and any previously described domain or sorting signal. It is unclear how these sequences direct its apical transport, but two models are proposed. First, the cytoplasmic determinant may be recognized by a cytosolic factor(s) that is responsible for forming apically targeted transport vesicles. This scenario has been proposed to be the mechanism underlying the sorting of several basolateral proteins. Interactions between basolateral sorting signals and cytosolic adaptor proteins result in a clustering of these membrane proteins in the TGN, which subsequently initiates the formation and the budding of the vesicles from the TGN (for review see Nelson, 1992). Second, the cytoplasmic tail of rhodopsin could be transported as a result of interacting with other apically targeted proteins. Further analysis is required to address this issue and distinguish these possibilities.

Our results suggest that rhodopsin is routed from the TGN to the apical surface via a direct pathway. Although a "retention" mechanism at the apical membrane is unlikely to be the primary cause of the apical localization of rhodopsin, whether it functions as an additional force to stabilize rhodopsin on the apical membrane is unclear. Interactions with the membrane cytoskeleton, for example, have been described in other systems as a means of anchoring proteins to a particular subcellular domain (Nelson and Veshnock, 1987; Hammerton et al., 1991).

Apical Targeting of Membrane-associated Protein GST–Rho39Tr in MDCK Cells

The trafficking of peripheral membrane-associated proteins is not understood as well as that of proteins proceeding through the ER–Golgi–TGN secretory pathway. Our observations that 20°C incubation reversibly blocks GST–Rho39Tr in a TGN-like compartment and that BFA treatment effectively alters GST–Rho39Tr transport indicate that this protein may be transported to the apical plasma membrane via the TGN along a similar pathway to that used for secretory or membrane proteins. A reversible 20°C block at the TGN and BFA effects have also been demonstrated in rhodopsin transport in MDCK cells using biochemical assays (Sung, C.-H., and J.-Z. Chuang, unpublished results).

The nonpalmitoylated GST–Rho39pal$^-$Tr was not found in the Golgi region, suggesting that the Golgi localization of GST–Rho39Tr is dependent on the palmitoylation signal and/or its resulting membrane anchor. Precedent examples have shown that acylation is required for targeting several membrane-associated proteins to their destined membrane domains, such as the Golgi apparatus. Moreover, such proper Golgi targeting appears to correlate with their subsequent correct subcellular targeting. For example, neuromodulin (GAP-43) is found to be associated with the Golgi apparatus (Van Hooff et al., 1989; Goslin et al., 1990) in addition to its growth cone localization (Zuber et al., 1989). Disruption of the palmitoylation signal at NH_2 terminus of GAP-43 abolishes its Golgi localization as well as its growth cone accumulation (Liu et al., 1997).

In order for GST–Rho39Tr to be effectively delivered to the apical surface of MDCK cells, the protein is likely to be processed and incorporated into membrane vesicles budding off the TGN through recognition of effector domains, presumably rhodopsin's cytoplasmic sequences. The data in the present study support this proposal. It is conceivable that GST–Rho39Tr is targeted to the cytoplasmic face of the Golgi membrane by affinity for palmitoyltransferase. Various palmitoyltransferase activities have been detected in several subcellular compartments, including the Golgi apparatus (Gutierrez and Magee, 1991). Alternatively, GST–Rho39Tr is palmitoylated before its Golgi targeting and subsequently interacts with the Golgi membrane via lipid–lipid or lipid–protein interactions.

If the palmitoylation signal simply acted as a Golgi-targeting signal, this would help to explain why the palmitoylation is not critical for the apical transport of the native rhodopsin protein, which already contains a signal sequence for transit through the ER–Golgi pathway. However, it is equally possible that the palmitoylation itself serves as a bona fide apical sorting signal on GST–Rho39Tr but is functionally redundant on rhodopsin. Further mutational analyses of rhodopsin are needed to distinguish these possibilities. Furthermore, we predict that either the palmitoyl moiety and/or rhodopsin's cytoplasmic sequences on GST–Rho39Tr further interact with the apical plasma membrane after its arrival, through lipid–lipid, lipid–protein, and/or protein–protein interactions. These interactions would stabilize GST–Rho39Tr on the apical membrane by preventing the lateral diffusion that is known to occur within the cytoplasmic plasma membrane leaflet (van Meer and Simons, 1986).

The Physiological Relevance of the Apical Targeting of Rhodopsin in MDCK Cells and in Photoreceptors

Dotti and Simons (1990) suggested that similar mechanisms are used in sorting proteins to the apical/basolateral surface of MDCK cells and to the axonal/dendritic regions of neuronal cells. However, a photoreceptor is more complicated in morphology and more compartmentalized than a conventional neuron, which has no counterpart to the cilium-derived outer segment. The topographic correlation between the apical membrane localization of rhodopsin in polarized MDCK cells and the initial "apical" inner segment plasma membrane targeting of rhodopsin (Papermaster and Schneider, 1982; Defoe and Besharse, 1985) is intriguing. Coincidentally, Na^+/K^+ ATPase, a molecule that accumulates basolaterally in most epithelia (Hammerton et al., 1991; Gottardi and Caplan, 1993), appears to be exclusively expressed in the "lateral plasma membrane" of the photoreceptor inner segment (Schneider and Kraig, 1990). Nevertheless, the question of whether studies of rhodopsin sorting in MDCK cells can be directly extrapolated to the photoreceptor remains open.

In summary, MDCK cells have proven be a useful model in studying the intracellular trafficking of many exogenously introduced proteins. In this report, we demon-

strate that the cytoplasmic amino acids of rhodopsin are able to act as an apical sorting signal in polarized MDCK cells. It is tempting to speculate that in MDCK cells a counterpart of the sorting mechanism used for basolateral proteins also exists for sorting some apical proteins, and our finding should provide a valuable resource to help identify essential components of the apical sorting receptor.

We thank Dr. R. Molday (University of British Columbia, Canada) for mAb 1D4, Dr. P. Hargrave (University of Florida, Gainesville, FL) for mAb B6-30, Dr. B. Seed (Massachusetts General Hospital, Boston, MA) for CD7 cDNA, Drs. Y.-T. Chen and W.J. Nelson (Stanford University, Stanford, CA) for a modified CD7BB plasmid, Drs. D.L. Price (Johns Hopkins University, Baltimore, MD) and M.F. Stinski (University of Iowa, Iowa City, IA) for pCB6 vector, and Dr. B. Chatton (LGME/CNRS, France) for pBC vector. We are grateful to Ms. Maria Eugene-Alfonzo and Ramee Lee for technical assistance and Dr. E. Rodriguez-Boulan, Dr. A. Musch, Dr. Huaxi Xu, Mr. A.W. Tai, and Ms. J. Macke for helpful discussion and advice on the manuscript.

This work was supported by grants to C.-H. Sung from the National Institutes of Health (NIH, EY11307), Research Preventing Blindness, and Cornell University Medical School institutional funding, and to J.-Z. Chuang from the NIH Tri-Institutional Training Program in Vision (EY07138).

Received for publication 20 April 1998 and in revised form 17 July 1998.

References

Adamus, G., A. Arendt, Z.S. Zam, J.H. McDowell, and P.A. Hargrave. 1988. Use of peptides to select for anti-rhodopsin antibodies with desired amino acid sequence specificities. *Pept. Res.* 1:42–47.

Applebury, M.L., and P.A. Hargrave. 1986. Molecular biology of the visual pigments. *Vision Res*. 26:1881–1895.

Arreaza, G., and A.D. Brown. 1995. Sorting and intracellular trafficking of a glycosylphosphatidylinositol-anchored protein and two hybrid transmembrane proteins with the same ectodomain in Madin-Darby canine kidney epithelial cells. *J. Biol. Chem.* 270:23641–23647.

Bacallao, R., C. Antony, C. Dotti, E. Karsenti, E.H.K. Stelzer, and K. Simons. 1989. The subcellular organization of Madin-Darby canine kidney cells during the formation of a polarized epithelium. *J. Cell Biol.* 109:2817–2832.

Balch, W.E., B.S. Glick, and J.E. Rothman. 1984. Sequential intermediates in the pathway of intercompartmental transport in a cell-free system. *Cell.* 39: 525–536.

Bomsel, M., K. Prydz, R.G. Parton, J. Gruenberg, and K. Simons. 1989. Endocytosis in filter-grown Madin-Darby canine kidney cells. *J. Cell Biol.* 109: 3243–3258.

Brown, D.A., B. Crise, and J.K. Rose. 1989. Mechanism of membrane anchoring affects polarized expression of two proteins in MDCK cells. *Science.* 245: 1499–1501.

Chatton, B., A. Bahr, J. Acker, and C. Kedinger. 1995. Eukaryotic GST fusion vector for the study of protein-protein associations *in vivo*: application to interaction of ATFa with Jun and Fos. *Biotechniques.* 18:142–145.

Defoe, D.M., and J.C. Besharse. 1985. Membrane assembly in retinal photoreceptors. II. Immunocytochemical analysis of freeze-fractured rod photoreceptor membranes using anti-opsin antibodies. *J. Neurosci.* 5:1023–1034.

Deretic, D., B. Puleo-Scheppke, and C. Trippe. 1996. Cytoplasmic domain of rhodopsin is essential for post-Golgi vesicle formation in a retinal cell-free system. *J. Biol. Chem.* 271:2279–2286.

Dotti, C.G., and K. Simons. 1990. Polarized sorting of viral glycoproteins to the axon and dendrites of hippocampal neurons in culture. *Cell.* 62:63–72.

Fiedler, K., and K. Simons. 1995. The role of N-glycans in the secretory pathway. *Cell.* 81:309–312.

Garcia-Cardena, G., P. Oh, J. Liu, J.E. Schnitzer, and W.C. Sessa. 1996. Targeting of nitric oxide synthase to endothelial cell caveolae via palmitoylation: implications for nitric oxide signaling. *Proc. Natl. Acad. Sci. USA.* 93:6448–6453.

Goslin, K., D.J. Schreyer, J.H. Skene, and G. Banker. 1990. Changes in the distribution of GAP-43 during the development of neuronal polarity. *J. Neurosci.* 10:588–602.

Gottardi, C.J., and M.J. Caplan. 1993. Delivery of Na^+, K^+-ATPase in polarized epithelial cells. *Science.* 260:552–554.

Grosenbach, D.W., D.O. Ulaeto, and D.E. Hruby. 1997. Palmitoylation of the vaccinia virus 37-kDa major envelope antigen. *J. Biol. Chem.* 272:1956–1964.

Gutierrez, L., and A.I. Magee. 1991. Characterization of an acyltransferase acting on p21N-ras protein in a cell-free system. *Biochim. Biophys. Acta.* 1078: 147–154.

Haller, C., and S.L. Alper. 1993. Nonpolarized surface distribution and delivery of human CD7 in polarized MDCK cells. *Am. J. Physiol.* 265:1069–1079.

Hammerton, R.W., K.A. Kizeminski, R.W. Mays, D.A. Wollner, and W.J. Nelson. 1991. Mechanism for regulating cell surface distribution of Na^+, K^+-ATPase in polarized epithelial cells. *Science.* 254:847–850.

Hodges, R.S., R.J. Heaton, J.M. Parker, L. Molday, and R. Molday. 1988. Antigen-antibody interaction: synthetic peptides define linear antigenic determinants recognized by monoclonal antibodies directed to the cytoplasmic carboxy terminus of rhodopsin. *J. Biol. Chem.* 263:11768–11775.

Hunziker, W., C. Harter, K. Matter, and I. Mellman. 1991. Basolateral sorting in MDCK cells requires a distinct cytoplasmic domain determinant. *Cell*. 66: 907–920.

Karnik, S.S., T.P. Sakmar, H.-B. Chen, and H.G. Khorana. 1988. Cysteine residues 110 and 187 are essential for the formation of correct structure in bovine rhodopsin. *Proc. Natl. Acad. Sci. USA*. 85:8459–8463.

Le Bivic, A., F.S. Real, and E. Rodriguez-Boulan. 1989. Vectorial targeting of apical and basolateral plasma membrane proteins in a human adenocarcinoma epithelial cell line. *Proc. Natl. Acad. Sci. USA*. 86:9313–9317.

Lisanti, M.P., A.L. Bivic, M. Sargiacomo, and E. Rodriguez-Boulan. 1989*a*. Steady-state distribution and biogenesis of endogenous Madin-Darby canine kidney glycoproteins: evidence for intracellular sorting and polarized cell surface delivery. *J. Cell Biol.* 109:2117–2127.

Lisanti, M.P., I.W. Caras, M.A. Davitz, and E. Rodriguez-Boulan. 1989*b*. A glycophospholipid membrane anchor acts as an apical targeting signal in polarized epithelial cells. *J. Cell Biol.* 109:2145–2156.

Liu, J., T.E. Hughes, and W.C. Sessa. 1997. The first 35 amino acids and fatty acylation sites determine the molecular targeting of endothelial nitric oxide synthase into the Golgi region of cells: a green fluorescent protein study. *J. Cell Biol.* 137:1525–1535.

Liu, Y., D.A. Fisher, and D.R. Storm. 1994. Intracellular sorting of neuromodulin (GAP-43) mutants modified in the membrane targeting domain. *J. Neurosci.* 14:5807–5817.

Low, S.H., B.L. Tang, S.H. Wong, and W. Hong. 1992. Selective inhibition of protein targeting to the apical domain of MDCK cells by brefeldin A. *J. Cell Biol*. 118:51–62.

Matlin, K.S., and K. Simons. 1983. Reduced temperature prevents transfer of a membrane glycoprotein to the cell surface but does not prevent terminal glycosylation. *Cell.* 34:233–243.

Mays, R., K.A. Siemers, B.A. Fritz, A.W. Lowe, G. van Meer, and W.J. Nelson. 1995. Hierarchy of mechanisms involved in generating Na/K-ATPase polarity in MDCK epithelial cells. *J. Cell Biol.* 130:1105–1115.

Mostov, K.E., A.B. Kops, and D.L. Deitcher. 1986. Deletion of the cytoplasmic domain of the polymeric immunoglobulin receptor prevents basolateral localization and endocytosis. *Cell.* 47:359–364.

Mostov, K.E., P. Breitfeld, and J.M. Harris. 1987. An anchor-minus form of the polymeric immunoglobulin receptor is secreted predominantly apically in Madin-Darby canine kidney cells. *J. Cell Biol.* 105:2031–2036.

Nelson, W.J. 1992. Regulation of cell surface polarity from bacteria to mammals. *Science.* 258:948–955.

Nelson, W.J., and P.J. Veshnock. 1987. Ankyrin binding to ($Na^+ + K^+$)ATPase and implications for the organization of membrane domains in polarized cells. *Nature.* 328:533–536.

Ojakian, G.K., R.E. Romain, and R.E. Herz. 1987. A distal nephron glycoprotein that has different cell surface distributions on MDCK cell sublines. *Am. J. Physiol.* 253:C433–C443.

Osawa, S., and E.R. Weiss. 1994. The carboxy-terminus of bovine rhodopsin is not required for G protein activation. *Mol. Pharmacol.* 46:1036–1040.

Papac, D.I., K.R. Thornburg, E.E. Bullesbach, R.K. Crouch, and D.R. Knapp. 1992. Palmitoylation of a G-protein coupled receptor. Direct analysis by tandem mass spectrometry. *J. Biol. Chem.* 267:16889–16894.

Papermaster, D.S., and B.G. Schneider. 1982. Biosynthesis and morphogenesis of outer segment membranes in vertebrate photoreceptor cells. *In* Cell Biology of the Eye. D.S. McDevitt, editor. Academic Press, New York. 477–531.

Prill, V., L. Lehmann, K. von Figura, and C. Peters. 1993. The cytoplasmic tail of lysosomal acid phosphatase contains overlapping but distinct signals for basolateral sorting and rapid internalization in polarized MDCK cells. *EMBO (Eur. Mol. Biol. Organ.) J.* 12:2181–2193.

Rodriguez-Boulan, E., and S.K. Powell. 1992. Polarity of epithelial and neuronal cells. *Annu. Rev. Cell Biol.* 8:395–427.

Roth, M.G., D. Gundersen, N. Patil, and E. Rodriguez-Boulan. 1987. The large external domain is sufficient for the correct sorting of secreted or chimeric influenza virus hemagglutinin in polarized monkey kidney cells. *J. Cell Biol.* 104:769–782.

Schmied, R., and E. Holtzman. 1989. Involvement of the Golgi apparatus in sorting of materials to opposite ends of frog rod retinal photoreceptors. *J. Neurobiol.* 20:115–138.

Schneider, B.G., and E. Kraig. 1990. Na, K-ATPase of the photoreceptor: selective expression of $\alpha 3$ and $\beta 2$ isoforms. *Exp. Eye Res.* 51:553–564.

Shenoy-Scaria, A.M., D.J. Dietzen, J. Kwong, D.C. Link, and D.M. Lublin. 1994. Cysteine 3 of Src family protein tyrosine kinase determines palmitoylation and localization in caveolae. *J. Cell Biol.* 126:353–363.

Simons, K., and A. Wandinger-Ness. 1990. Polarized sorting in epithelia. *Cell.* 62:207–210.

Sullivan, L.S., and S.P. Daiger. 1996. Inherited retinal degeneration: exceptional genetic and clinical heterogeneity. *Mol. Med. Today.* 2:380–386.

Sung, C.-H., B.G. Schneider, N. Agarwal, D.S. Papermaster, and J. Nathans. 1991. Functional heterogeneity of mutant rhodopsins responsible for autosomal dominant retinitis pigmentosa. *Proc. Natl. Acad. Sci. USA.* 88:8840–8844.

Sung, C.-H., C. Makino, D. Baylor, and J. Nathans. 1994. A rhodopsin gene mutation responsible for autosomal dominant retinitis pigmentosa results in a protein that is defective in localization to the photoreceptor outer segment. *J. Neurosci.* 14:5818–5833.

Van Hooff, C.O., J.C. Holthuis, A.B. Oestreicher, J. Boonstra, P.N. De Graan, and W.H. Gispen. 1989. Nerve growth factor–induced changes in the intracellular localization of the protein kinase C substrate B-50 in pheochromocytoma PC12 cells. *J. Cell Biol.* 108:1115–1125.

van Meer, G., and K. Simons. 1986. The fusion of tight junctions in maintaining differences in lipid composition between the apical and the basolateral cell surface domains of MDCK cells. *EMBO (Eur. Mol. Biol. Organ.) J.* 5:1455–1464.

van't Hof, W., and M.D. Resh. 1997. Rapid plasma membrane anchoring of newly synthesized $p58^{fyn}$: selective requirement for NH_2-terminal myristoylation and palmitoylation at cysteine-3. *J. Cell Biol.* 136:1023–1035.

Wandinger-Ness, A., M.K. Bennett, C. Antony, and K. Simons. 1990. Distinct transport vesicles mediate the delivery of plasma membrane proteins to the apical and basolateral domains of MDCK cells. *J. Cell Biol.* 111:987–1000.

Wedegaertner, P.B., P.T. Wilson, and H.R. Bourne. 1995. Lipid modifications of trimeric G proteins. *J. Biol. Chem.* 270:503–506.

Yeaman, C., A.H. Le Gall, A.N. Baldwin, L. Monlauzeur, A. Le Bivic, and E. Rodriguez-Boulan. 1997. The *O*-glycosylated "stalk" domain is required for apical sorting of neurotrophin receptors in polarized MDCK cells. *J. Cell Biol.* 139:929–940.

Zuber, M.X., S.M. Strittmatter, and M.C. Fishman. 1989. A membrane-targeting signal in the amino terminus of the neuronal protein GAP-43. *Nature.* 341:345–348.